Journal of Materials Chemistry

Cite this: J. Mater. Chem., 2011, 21, 11205

www.rsc.org/materials

View Online
Dynamic Article Links

PAPER

A fifteen atom silver cluster confined in bovine serum albumin†

Ammu Mathew, P. R. Sajanlal and T. Pradeep*

Received 6th April 2011, Accepted 17th May 2011
DOI: 10.1039/c1jm11452b

Downloaded by Indian Institute of Technology Chennai on 11 September 2011
Published on 23 June 2011 on http://pubs.rsc.org | doi:10.1039/C1JM11452B

Luminescent Ag_{15} clusters confined in bovine serum albumin (BSA) have been prepared by a simple wet chemical route. The luminescence, exhibiting a maximum at 685 nm, is observable to the naked eye. The chemical composition of these clusters was analyzed using matrix assisted laser desorption ionization mass spectrometry (MALDI MS), X-ray photoelectron spectroscopy (XPS), and energy dispersive analysis of X-rays (EDAX). Intact Ag_{15}@BSA is observed by MALDI MS. Multiple charge states of the cluster are observed confirming the mass assignment. The clusters showed a quantum yield of 10.71% in water and the luminescence was stable in a pH range of 1–12. Stability of the clusters was enhanced by the addition of polyvinylpyrrolidone (PVP). The clusters showed luminescence in the solid state as well. Evolution of clusters with variation in the amount of reducing agent added shows that the cluster formation goes through an intermediate state of bound silver, formed instantaneously after the addition of Ag^+, which transforms to the cluster. High yield synthesis and exciting photophysical properties make our new material interesting for various applications such as biolabeling and imaging.

Introduction

The study of few-atom metal clusters (or quantum clusters) is an active area of recent research as they bridge the evolution of properties of materials from isolated atoms to nanoparticles (NPs)[1,2] and triggers a wide variety of possible applications in the fields of catalysis,[3–5] biolabelling,[6–8] optical sensing,[6] *etc.* Extremely small size, good photostability[8] (compared to traditional organic dyes), better quantum efficiency,[6,9] low toxicity[10] and excellent photoluminescence quantum yield make them suitable for biological applications.[11] Several such clusters of noble metals have been synthesized using various templates such as peptides,[12] thiols,[2,13–15] dendrimers,[16] proteins,[6,17–22] polymers,[23,24] and DNA.[25–27] Among them, the use of a biomolecule as template or scaffold for synthesis possesses many advantages in biological applications.[28]

Silver clusters are more reactive than their gold analogues. Consequently, limited reports exist on them. However, various methods have been reported for the preparation of Ag clusters[2] and many of them are highly luminescent both in solution and solid states. Among them Ag clusters synthesized *via* gas-phase and low-temperature matrix-isolation methods[29] were the first to show discrete absorption and fluorescence. Chemiluminescence due to the formation of excited Ag_2 and Ag_3 clusters during Ag condensation with Ar has also been reported.[30] Non-luminescent silver clusters have been observed in frozen solutions and zeolites.[31] Various methods such as radiolytic reduction,[24,32] sonochemical synthesis,[22,33] chemical reduction,[14,19,26,27,34] photoreduction,[35] *etc.* have also been used for making Ag clusters. A solid state route for the synthesis of Ag_9 cluster has been developed recently by our group.[14] We have also made silver clusters by following an interfacial method.[36,37]

As the silver clusters are prone to aggregation and grow to form larger clusters/nanoparticles, so as to reduce their surface energy, it is necessary to have some pre-formed templates or capping agents to synthesize stable entities.[28] The use of biomolecules as protecting agents is a step towards developing green chemistry protocols for making quantum clusters. Besides, it allows the clusters to penetrate easily into cells and help monitor fundamental life processes such as replication of DNA and other genomic events. Due to their luminescence property, individual molecular events that are happening inside the cells can be visualized, measured, and tracked using fluorescence microscopy. BSA is a well studied protein and has long been used as a capping agent for making nanoparticles due to its strong affinity towards inorganic salts.[38,39] As in the case of dendrimers, the cage effect of the protein stabilizes the clusters and enhances their optical properties. This caging may prevent their photodecomposition. Our group has recently synthesized Au_{15} quantum clusters partially encapsulated in α-, β-, and γ-cyclodextrin (CD) cavities.[40] Luminescent clusters have been embedded also in silica shells.[41] Xie *et al.*[17] synthesized highly

DST Unit of Nanoscience (DST UNS), Department of Chemistry, Indian Institute of Technology Madras, Chennai, 600 036, India. E-mail: pradeep@iitm.ac.in

† Electronic supplementary information (ESI) available: Emission spectra of Ag15@BSA at different pH, MALDI MS of control experiments, XPS spectrum of Ag_{15}@BSA, luminescence profile of Ag_{15}@BSA solid, fluorescence lifetime data of Ag_{15}@BSA, absorption and emission profiles showing the effect of solvents on the formation of the cluster, absorption spectra, emission profiles and MALDI MS data of Ag_{15}@BSA during decomposition at 28 °C and at 10 °C. See DOI: 10.1039/c1jm11452b

This journal is © The Royal Society of Chemistry 2011

View Online

Downloaded by Indian Institute of Technology Chennai on 11 September 2011
Published on 23 June 2011 on http://pubs.rsc.org | doi:10.1039/C1JM11452B

luminescent gold QCs using the reduction capacity of BSA at pH 12. Luminescent QCs of gold with a quantum yield of ~4% were synthesized from AuNPs by using BSA as an etching agent.[6] Recently Liu *et al.* synthesized BSA protected Au and Au@Ag clusters using a sonochemical approach.[22]

Herein, we report the synthesis of BSA protected fifteen atom clusters of silver using a rapid, room-temperature synthetic protocol. The resulting bright red emitting clusters were assigned a molecular formula based on MALDI MS. BSA was chosen for the present study owing to its stability and non-reactivity in many biochemical reactions as well as low cost and effectiveness in forming such clusters.[17] The clusters were characterized thoroughly using various spectroscopic and microscopic techniques. The effect of reducing agent on the luminescence property of the resulting cluster solution was probed. Several control experiments were done in order to verify the formation of clusters and a possible mechanism of their formation has been proposed.

Experimental

Materials

Silver nitrate ($AgNO_3$) and sodium hydroxide (NaOH) were purchased from Rankem, India. BSA and poly(*N*-vinyl-2-pyrrolidone) (K_{60}) were purchased from Sisco Research Laboratories. Sodium borohydride ($NaBH_4$) was purchased from Spectrochem, India. All chemicals were of analytical grade and were used without further purification. Triply distilled water was used throughout the experiments.

Synthesis of Ag_{15}@BSA

Ag_{15}@BSA was synthesized using a modified procedure of that used by Xie *et al.*[17] for the synthesis of Au_{25} clusters in BSA matrix. In a typical synthesis, 5 mL of 10 mM silver nitrate solution was added to 250 mg BSA powder in 5 mL distilled water with vigorous stirring at room temperature. About 0.3 mL NaOH (1 M) was added followed by 10 mM $NaBH_4$ solution drop-wise until the solution turns from colourless to reddish brown, indicating the formation of various amounts of clusters. Controlled addition of $NaBH_4$ in the above step can yield solutions with tunable luminescence from green to red, when observed under UV light.

Instrumentation

Scanning electron microscopic (SEM) images and EDAX images were obtained using a FEI QUANTA-200 SEM. For the SEM and EDAX measurements, samples were spotted on an indium tin oxide (ITO) conducting glass substrate and dried in ambient condition. Transmission electron microscopy (TEM) was carried out using a JEOL 3011, 300 kV instrument with an ultra high resolution (UHR) pole piece. The samples for TEM were prepared by dropping the dispersion on amorphous carbon films supported on a copper grid and dried. MALDI MS studies were conducted using a Voyager DE PRO Biospectrometry Workstation (Applied Biosystems) matrix assisted laser desorption ionization time-of-flight mass spectrometer (MALDI TOF MS). A pulsed nitrogen laser of 337 nm was used (maximum firing rate, 20 Hz; maximum pulse energy, 300 μJ) for the MALDI MS studies. Mass spectra were collected in positive mode and were averaged for 100 shots. Sinapic acid was used as the matrix for MALDI MS. Optical absorption spectra were collected using a Perkin-Elmer Lambda 25 spectrophotometer. The experiments were carried out at room temperature and the absorption spectra were recorded from 200 to 1100 nm. Luminescence measurements were carried out on a Jobin Yvon NanoLog instrument. The bandpass for excitation and emission was set as 5 nm. XPS measurements were conducted with an Omicron ESCA Probe spectrometer with polychromatic Mg Kα X-rays ($h\nu$ = 1253.6 eV). The samples were spotted as drop-cast films on a sample stub. A constant analyzer energy of 20 eV was used for the measurements. Fluorescence transients were measured and fitted using a commercially available spectrophotometer (Life-Spec-ps, Edinburgh Instruments, UK) having an 80 ps instrument response function.

Results and discussion

Silver clusters conjugated to BSA were synthesized in aqueous solution at room temperature using sodium borohydride as the reducing agent. Clusters were formed rapidly just after the addition of a reducing agent to a solution containing Ag^+ ions, BSA and NaOH. Here, BSA stabilizes the clusters and provides steric protection due to its bulkiness. BSA is composed of 583 amino acid residues of which 35 are cysteine and 5 are methionine. Addition of silver nitrate solution to aqueous BSA causes the silver ions to be coordinated to the various functional groups of BSA such as –NH, –OH, and –SH, and they are subsequently reduced to clusters by the addition of $NaBH_4$ at alkaline pH. Experiments conducted in neutral and acidic pH did not result in the clusters. The pH of the solution was adjusted to 12 by the addition of NaOH as BSA is known to act as a reducing agent[42] as well as/or capping agent in alkaline medium.[17] Addition of $NaBH_4$ into a solution containing BSA, $AgNO_3$ and NaOH at room temperature under vigorous stirring changes the colour of the solution from colourless to golden yellow and finally to light brown, indicating the formation of the clusters. The light brown solution showed bright red luminescence under UV light. Formation of clusters was first characterized by UV-vis absorption spectroscopy. Fig. 1A compares the absorption spectra of pure BSA solution (black trace) and the red emitting cluster, Ag_{15}@BSA (red trace, the cluster nuclearity is discussed below). A decrease in intensity of the characteristic absorption of BSA at 279 nm was observed in the case of Ag_{15}@BSA. The cluster solution also showed a broad absorption peak from 380 to 680 nm with small humps at 415 and 485 nm. The molar extinction coefficients for the cluster features were calculated as 1204.1 L mol^{-1} cm^{-1} (279 nm), 59.0 L mol^{-1} cm^{-1} (415 nm) and 38.6 L mol^{-1} cm^{-1} (485 nm). The inset of Fig. 1A shows an expanded view of the spectra in which the cluster features (marked with arrows) and the onset of absorption at 680 nm (marked with dotted arrow) are shown. These features were not observed in BSA and could be characteristic of the cluster. The well-defined molecular transitions associated with thiolate protected Ag clusters[14] or other red luminescent noble metal quantum clusters[43] were not seen in this case as these clusters are well protected by the bulky BSA. Fig. 1B shows the luminescence profile of the as-prepared red emitting Ag_{15}@BSA. The cluster

 This journal is © The Royal Society of Chemistry 2011

View Online

Downloaded by Indian Institute of Technology Chennai on 11 September 2011
Published on 23 June 2011 on http://pubs.rsc.org | doi:10.1039/C1JM11452B

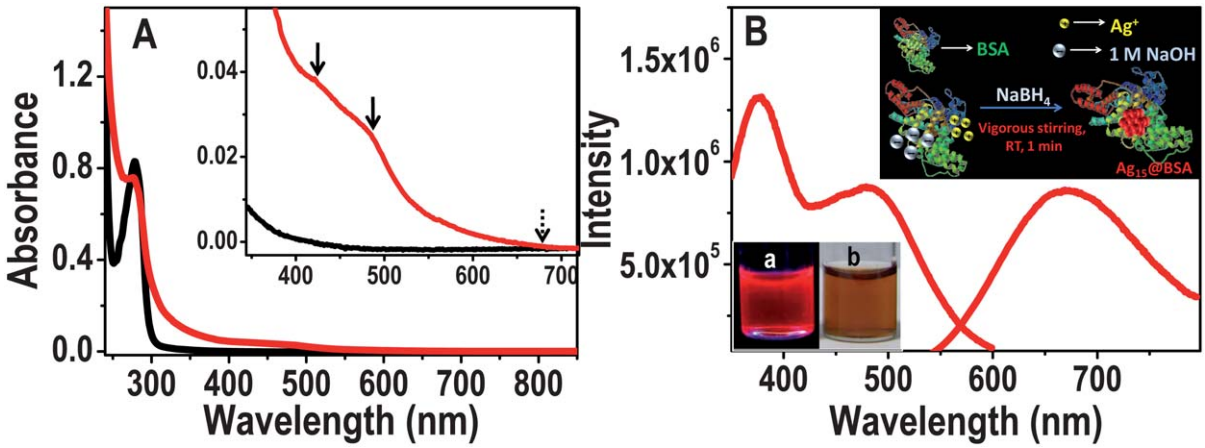

Fig. 1 (A) UV-vis absorption spectra of the red emitting Ag_{15}@BSA clusters (red trace) and that of pure BSA (black trace). The inset of A is an enlarged view of the spectra showing the onset of absorption at 680 nm (marked with a dotted arrow). The cluster features observed at 415 and 485 nm are marked using solid arrows. (B) Luminescence profile of the as-prepared Ag_{15}@BSA. The inset of B contains the photographs of the clusters under UV light (a) and under visible light (b). Schematic of the experimental procedure employed for the preparation of Ag_{15}@BSA is shown in the inset of B.

solution in water showed a bright red emission centred around 685 nm with two excitation peaks around 380 and 480 nm. The quantum yield of the cluster was calculated to be 10.71% in water using fluorescein as the reference. This was much higher than that reported for BSA protected gold cluster (~6%).[17] The photographs of the cluster solution under UV and visible radiations are shown in the inset of Fig. 1B. The luminescence was stable in the pH range of 1–12 (Fig. S1A†). The inset of Fig. 1B also shows a schematic of the cluster synthesis.

The nuclearity of Ag@BSA clusters was studied using MALDI MS (Fig. 2). BSA showed a broad mass peak around *m*/*z* 66.7 kDa and the as-prepared cluster showed a peak around *m*/*z* 68.3 kDa. The difference corresponds to 15 atoms of Ag. The presence of doubly as well as triply charged clusters along with the corresponding peaks of the protein observed in the MALDI MS spectrum clearly indicates that the metal cluster is associated with a single protein molecule (Fig. 2). All of these peaks also have almost similar intensities as in the free protein, which also

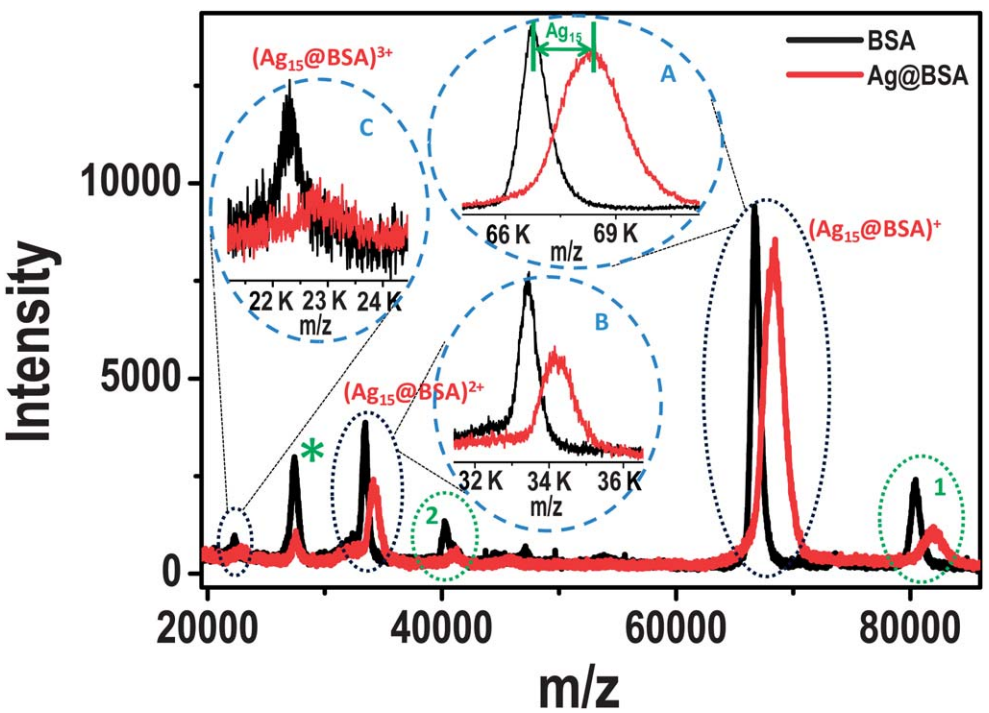

Fig. 2 MALDI MS of pure BSA solution (black trace) collected in linear positive ion mode using sinapic acid as matrix and that of the as-prepared red emitting Ag_{15}@BSA (red trace). The peaks due to singly, doubly and triply charged ions of Ag_{15}@BSA are expanded in the inset marked A, B and C, respectively. Peaks marked 1 and 2 are singly and doubly charged species of conalbumin which is an internal standard used in BSA protein. The impurity peak at *m*/*z* 27.5 kDa is marked with an '*'.

View Online

Downloaded by Indian Institute of Technology Chennai on 11 September 2011
Published on 23 June 2011 on http://pubs.rsc.org | doi:10.1039/C1JM11452B

supports this argument. These peaks are expanded separately as insets in the same figure. All of these peaks also support the same cluster core. In view of all these, we assign the cluster as Ag_{15}@BSA. No other cluster was detected. We found yet another peak around *m*/*z* 80 kDa which can be attributed to the protein conalbumin, an internal standard used in BSA protein.[44] Singly and doubly charged (around *m*/*z* = 40 kDa) species of this are marked in Fig. 2. These features were present in MALDI MS of both BSA as well as in the cluster. These peaks in the cluster sample were shifted to higher mass, corresponding to 15 atoms of silver, possibly due to the formation of clusters inside this protein as well. The peak at *m*/*z* 27.5 kDa (marked with an *) does not show any shift and is attributed to an impurity.

In order to confirm the formation of clusters, we performed several control experiments. Solutions of various combinations of the reagents used for cluster synthesis were prepared and analyzed using MALDI MS. The mass spectra of pure BSA (i), mixture of BSA and $AgNO_3$ (ii), mixture of BSA, $AgNO_3$ and NaOH (iii), and mixture of BSA, NaOH and $NaBH_4$ (iv) are shown in Fig. S1B†. No drastic shift was observed in the case of (iv) when compared to pure BSA (i) which proves that the observed shift in mass spectra for red emitting clusters (Fig. 2) was due to the addition of Ag atoms into the BSA scaffold and not due to any possible structural change induced by the addition of sodium borohydride at alkaline pH. The slight shift observed in the case of (ii) and (iii) when compared to (i) is due to the coordination of the silver ions to the protein matrix because of the presence of various functional groups such as –NH and –SH on the protein.

The chemical composition of the clusters was further confirmed using EDAX. The EDAX spectrum of the Ag_{15}@BSA is shown in Fig. 3A. The inset of A gives the quantification data of the solid cluster. An approximate ratio of Ag : S in the cluster is 2.33 which is in good agreement with the theoretical value (2.66) by assuming that one Ag_{15} cluster is present per BSA molecule. Note that BSA contains 40 sulfur atoms due to 35 cysteine and 5 methionine units. Fig. 3C–E are the EDAX images collected using Ag Lα, S Kα and N Kα, respectively. The corresponding SEM image of the sample is shown in Fig. 3B. The chemical composition of Ag_{15}@BSA was verified by XPS. Fig. S2† gives the XPS spectrum in the Ag 3d region. The observed peaks of Ag $3d_{5/2}$ and Ag $3d_{3/2}$, at ~368.2 and ~374.3 eV, respectively confirm the existence of silver in its zero valent form.

These clusters were freeze dried into powder form and the powders also showed luminescence at room temperature. We could also solidify the clusters by evaporating the solvent from the cluster solution by subjecting it to flowing hot air. The freeze dried solid Ag_{15}@BSA showed almost 39% decrease in its luminescence intensity compared to that solidified under flowing hot air. This indicates that the as prepared red emitting clusters are stable even on increasing the temperature to 50–60 °C, provided the evaporation is rapid. At the same time, slow heating of the cluster solution at 50 °C for 30 min resulted in their decomposition. Fig. S3† shows the luminescence profiles of the solidified silver clusters along with the photographs of the freeze dried sample. Due to the better luminescence of the hot air dried sample compared to the freeze dried solid, the former was used for further studies. Photographs of the former sample in visible light and UV light are given in Fig. 4A and B.

The cluster emissions in both solution and solid state decreased with time when exposed to ambient air at room temperature. The stability of the as formed Ag_{15}@BSA enhanced considerably by the addition of 1 mL of 2.5 mg mL^{-1} PVP (to 10.42 mL as-prepared cluster solution). PVP is known to coordinate weakly with metal clusters and thereby increase their stability.[45,46] The luminescence property of the PVP stabilized Ag_{15}@BSA kept at room temperature remained almost unchanged even after one week. Photographs of the bright red emitting solid, Ag_{15}@BSA, prepared without (A and B) and with (C and D) PVP are shown in Fig. 4. In both the cases, solid Ag cluster showed an intense red luminescence.

Fig. 4E shows the excitation and emission spectra of solid Ag_{15}@BSA with and without PVP protection at 0 h and after 24 h. The same samples were kept at room temperature and analysed after 24 h. Both the solid cluster samples showed an excitation with the peak maximum around 510 nm. From the luminescence profiles, an 82% decrease in the luminescence intensity was observed after 24 h for Ag_{15}@BSA without PVP

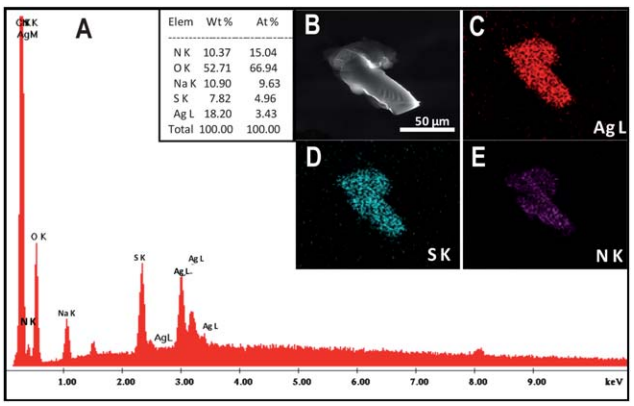

Fig. 3 The EDAX spectrum of the Ag_{15} cluster along with the quantification data (A). (C–E) are the EDAX images of the cluster collected using Ag Lα, S Kα, and Na Kα emissions. Corresponding SEM image of the Ag_{15}@BSA is shown in B. The quantification data suggest that the Ag : S ratio is in good agreement with the theoretical value.

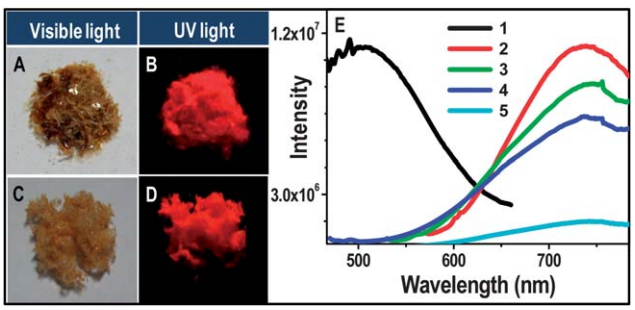

Fig. 4 (A and B) are the photographs of the Ag_{15}@BSA solid without PVP in visible light and UV light, respectively. (C and D) are the corresponding photographs of the Ag_{15}@BSA solid after the addition of PVP. (E) Luminescence profiles of the solid cluster showing the effect of addition of PVP on its stability. Trace 1 is the common excitation at 510 nm and traces 2–5 are emission spectra of solid Ag@BSA, solid Ag@BSA after the addition of PVP, PVP stabilized solid Ag@BSA after 24 h, and pure solid Ag@BSA after 24 h, respectively.

 This journal is © The Royal Society of Chemistry 2011

View Online

Downloaded by Indian Institute of Technology Chennai on 11 September 2011
Published on 23 June 2011 on http://pubs.rsc.org | doi:10.1039/C1JM11452B

protection when compared to freshly prepared sample whereas only 24% decrease was observed after PVP protection. Thus addition of PVP to the cluster not only enhances the stability of the system but also retains its characteristic emission feature. Even after the addition of PVP, there was no considerable shift in the luminescence profile which indicates that the clusters are intact inside BSA which in turn is stabilized by PVP. The observed shift in the excitation and emission wavelengths of the solid clusters with and without PVP when compared to the parent cluster solution can be attributed to the confinement of the cluster in the solid state.

The fluorescence decay of Ag_{15}@BSA was measured using a picosecond resolved, time-correlated single-photon-counting (TCSPC) technique. The decay profile of the cluster was monitored at an excitation wavelength of 445 nm (Fig. S4†). Lifetimes of the cluster are 0.28 ns (60%), 1.17 ns (30%) and 4.10 ns (10%).

The amount of reducing agent plays an important role in the formation of clusters. By controlled addition of $NaBH_4$, we were able to isolate intermediate stages during the synthesis. These solutions showed different colours under UV light indicating the possibility of tuning the apparent luminescence of the clusters from blue to red in the visible spectrum. Fig. 5A shows the photograph taken under UV light and visible light of various Ag cluster solutions isolated after the controlled addition of $NaBH_4$. Luminescence profiles of the corresponding solutions are shown in Fig. 5B. Pure BSA solution showed a blue luminescence under UV light (bottle 1 in Fig. 5A) with excitation and emission maxima of 290 and 345 nm, respectively. The black trace in Fig. 5B shows the emission spectrum of BSA. After the addition of $AgNO_3$ and NaOH to the BSA solution, emission of BSA was shifted from 345 nm to 445 nm (red trace in Fig. 5B) and its colour under UV light changed to green (bottle 2 in Fig. 5A). This observed red shift in the emission maximum from pure BSA can probably be attributed to the coordination of silver ions to the BSA matrix. Henceforth this green emitting species is referred to as Ag–BSA conjugate. Addition of 0.010 mL of 10 mM $NaBH_4$ into the above solution was observed to shift the peak maximum slightly to 456 nm (green trace in Fig. 5B) with an excitation at 380 nm. The resulting solution also showed a green luminescence under UV light (bottle 3 in Fig. 5A). As the amount of $NaBH_4$ added was increased, luminescence of the solution under UV lamp also underwent a sequential change in the order green, yellow, orange, and finally red. We studied the emission profiles of these solutions at two excitation wavelengths (380 and 480 nm) which were observed for the red emitting clusters (see Fig. 1B). When the emission spectra of the solutions were measured for an excitation wavelength of 480 nm, only the peak at 685 nm was observed which was increasing in its intensity with increase in $NaBH_4$ added to the mixture during synthesis. Whereas the excitation of various cluster solutions at 380 nm enabled simultaneous observation of two emission features at 455 and 685 nm. Interestingly, the luminescence profile of the different samples isolated at various stages of the reaction after the addition of $NaBH_4$ did not show any shift in its emission wavelength at 455 nm, though the colour of the solutions underwent a significant change from blue (BSA solution) to green, yellow, orange and finally to red under the UV lamp. As the amount of $NaBH_4$ in the solution was increased slowly, a new peak with a peak maximum at 685 nm emerged and the intensity of the peak at 455 nm decreased (marked with arrows in the figure). A distinct isoemission point was observed at 555 nm. This systematic change in emission spectra could be attributed to the formation of more red emitting clusters upon addition of $NaBH_4$. These red emitting clusters were characterised earlier as Ag_{15}@BSA. Addition of a small amount of $NaBH_4$ (0.010 mL) to the mixture of $AgNO_3$, BSA and NaOH (bottle 3 in Fig. 5A) did not cause any significant change in the luminescence of the solution under UV lamp as the amount of red emitting clusters that formed was much less. Thus the solution has two species, a red emitting cluster and the green emitting Ag–BSA conjugate.

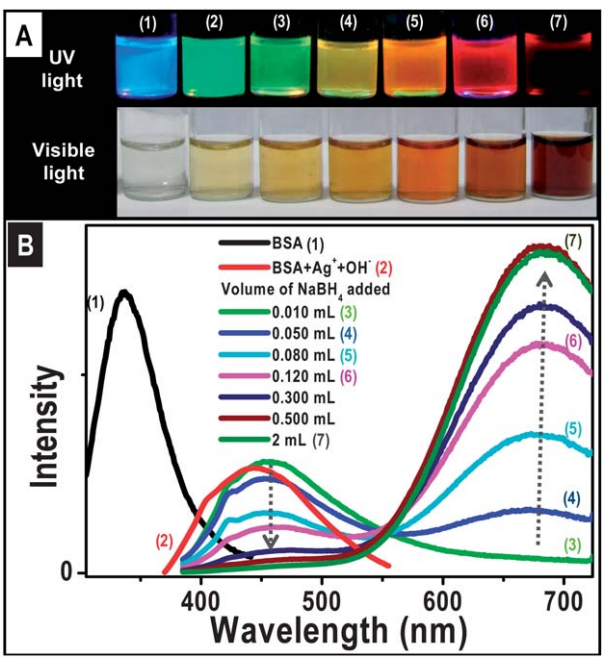

Fig. 5 (A) Photographs of the various solutions prepared during controlled addition $NaBH_4$ under UV light and visible light. (B) Emission spectra of the corresponding solutions. Emission spectra of pure BSA solution (black trace) and of the mixture of $AgNO_3$, BSA, and NaOH (green trace) are also shown.

The combined effect of the green luminescence of Ag–BSA conjugate and the increasing amount of red emitting Ag_{15}@BSA formed in the solution is therefore responsible for the gradual variation in the colours observed under UV light. When excess $NaBH_4$ (2 mL) was added during synthesis, the colour of the solution became dark brown under visible light and the luminescence appeared to be quenched under UV light as shown in Fig. 5A (bottle 7). However, there was no decrease in the intensity of the peak at 685 nm (Fig. 5B). Although clusters are formed, the luminescence appeared quenched under UV light as larger nanoparticles absorb light strongly. The TEM image of Ag clusters synthesized at the optimized condition (0.12 mL, 10 mM $NaBH_4$) did not show the signature of any nanoparticles (Fig. 6A) whereas those synthesized with the addition of excess $NaBH_4$ (2 mL) showed the presence of nanoparticles as shown in Fig. 6B. Here, nanoparticles of size greater than 5 nm are observed along with the clusters. The inset of Fig. 6B shows one such nanoparticle of 5 nm diameter. We did not observe any electron beam induced nanoparticle formation, a common phenomenon in the case of monolayer protected clusters,[47]

View Online

Downloaded by Indian Institute of Technology Chennai on 11 September 2011
Published on 23 June 2011 on http://pubs.rsc.org | doi:10.1039/C1JM11452B

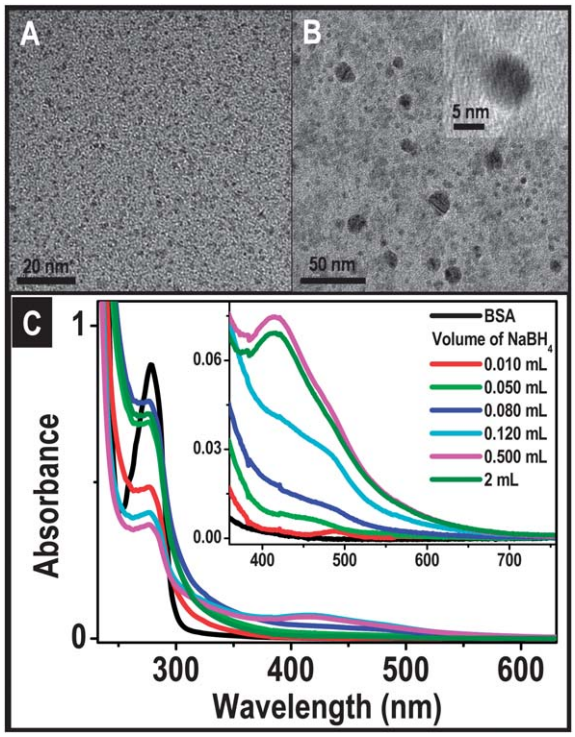

Fig. 6 TEM images of (A) Ag_{15}@BSA cluster prepared using optimized concentration of $NaBH_4$. The dark spots seen may be aggregates of the clusters. (B) Nanoparticles of size >5 nm formed as a result of addition of excess $NaBH_4$ (2 mL) during synthesis. The inset shows a single nanoparticle of ~5 nm diameter. Due to the presence of a protein shell, sharpness of the cluster in the TEM image got reduced. (C) UV-vis absorption spectra of the solutions illustrating the effect of addition of $NaBH_4$ to the solution during the synthesis of the cluster. Absorption spectrum of pure BSA solution (black trace) is also shown. The inset of C is an expanded view of the spectra.

probably due to the fact that the clusters are well-protected inside the protein shell. UV-vis absorption spectra of the different samples isolated after addition of $NaBH_4$ are shown in Fig. 6C.

With the addition of $NaBH_4$, characteristic absorption features of the red emitting Ag_{15}@BSA emerged gradually. Upon addition of 2 mL $NaBH_4$, a prominent absorption feature centred around 411 nm was observed which can be attributed to nanoparticles formed in the solution along with the clusters. Rapid addition of $NaBH_4$ into the solution containing the metal ions is likely to reduce silver ions to nanoparticles, but in our case the presence of protein acts as a scaffold which protects the clusters and prevents its growth into nanoparticles to a large extent.

The various cluster solutions isolated as described above were further characterized by MALDI MS to see whether new clusters are formed. Fig. 7 shows the mass spectra of the solutions collected after the addition of various amounts of $NaBH_4$. Addition of Ag^+ and NaOH to BSA results in a shift in the mass spectrum of BSA as shown in Fig. S1B†. After the addition of 10 μL of $NaBH_4$, the intensity of the MALDI feature corresponding to 15 atom silver cluster was weak (light green trace of Fig. 7). This feature increased upon successive addition of $NaBH_4$. From this we infer that red emitting Ag_{15}@BSA is the major component formed during the reaction, though various other clusters

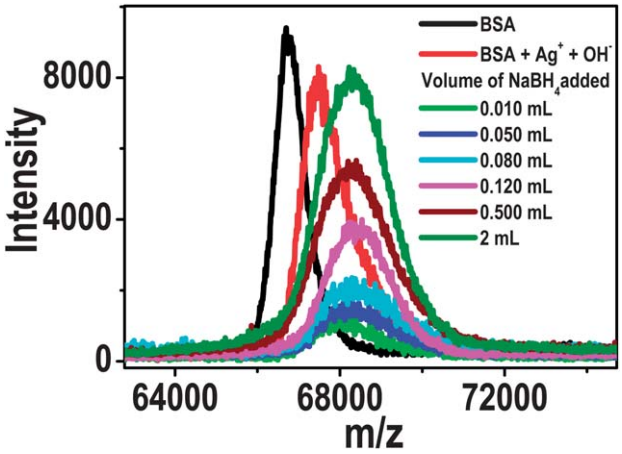

Fig. 7 MALDI MS collected in linear positive ion mode of the various solutions separated during the addition of $NaBH_4$ to the solution during the synthesis of clusters. Mass spectra of pure BSA solution (black trace) and that of a mixture of BSA, $AgNO_3$ and NaOH (red trace) are also shown for comparison. Beyond 2 mL $NaBH_4$, no further change is seen.

are also possible. There is no other major product in the reaction, especially when the reductant concentration is large. These results also validate the possibility of formation of a mixture of red emitting clusters and green emitting Ag–BSA conjugate. As no other product is likely, increase in BH_4^- only helps in the conversion of Ag–BSA conjugate to clusters. Beyond 2 mL BH_4^-, no further change is seen indicating complete reduction.

In order to study the solvent dependency of cluster formation, experiments were conducted in different solvents such as ethanol and acetonitrile. Fig. S5† shows the effect of solvents on the formation of red emitting clusters. The UV-vis absorption profile of the solutions (Fig. S5A†) showed no drastic variation when ethanol was used as the solvent instead of water in cluster synthesis. But an increase in absorbance of the peak at 480 nm was noted when acetonitrile was used as the solvent (inset of Fig. S5A†). The luminescence profiles of the clusters prepared in different solvents were also measured. Ag_{15}@BSA prepared using acetonitrile as solvent showed higher emission intensity (green trace in Fig. S5B†) compared to those prepared using water and ethanol as solvent. A slight red shift in emission intensity was also observed indicating the possibility of minor increase in the size of the clusters. From these data, we concluded that solvent has some influence on the luminescence intensity of the Ag cluster. This may be due to the conformational change of the BSA scaffold in solvents of different polarities.

We also probed the stability of these clusters at various temperatures. The decomposition profile of the red emitting Ag_{15}@BSA cluster solution without the addition of any stabilization agent was studied at room temperature (28 °C) and at 10 °C by UV-vis absorption spectroscopy, photoluminescence spectroscopy, and MALDI MS. Fig. S6† shows the luminescence profile of the samples at various time intervals such as 0, 7, 15 and 30 h at 28 °C (Fig. S6A†) and at 10 °C (Fig. S6B†), respectively.

The luminescence profiles of the cluster solution at 28 °C showed a drastic decrease in the emission intensity at 685 nm with time. After 20 h of incubation at 28 °C, the cluster solution exhibited a weak red luminescence under UV light but after 30 h,

 This journal is © The Royal Society of Chemistry 2011

View Online

Downloaded by Indian Institute of Technology Chennai on 11 September 2011
Published on 23 June 2011 on http://pubs.rsc.org | doi:10.1039/C1JM11452B

the solution showed a green luminescence. This change in luminescence may be attributed to the decomposition of Ag_{15}@BSA into Ag–BSA conjugate. Fig. S6A† shows the luminescence decay profile of Ag_{15}@BSA solution at 28 °C. The disappearance of the peak at 685 nm and appearance of a peak at 455 nm with time were observed. The reason is as mentioned above. The resultant spectrum after 30 h was almost the same as that of Ag–BSA conjugate (Fig. 5B). A plot of emission intensity of the feature at 455 nm (Ag–BSA conjugate) *versus* amount of $NaBH_4$ added shows a gradual disappearance of the feature observed at 455 nm (Fig. S6E†). Room temperature (28 °C) decay of the cluster with time (Fig. S6E†) showed a gradual increase of the same feature probably due to the formation of the conjugate. In contrast, the luminescence profile of the cluster solution incubated at 10 °C (Fig. S6B†) remained almost unchanged in its luminescence intensity up to a period of 30 h. UV-vis absorption spectroscopic studies of the two solutions at various time intervals (0, 6, 15 and 30 h) showed a drastic decay of the cluster features in the case of the solution kept at 28 °C (Fig. S6C†). The solution showed an almost featureless absorption after 30 h. In comparison, the solution incubated at 10 °C (Fig. S6D†) retained the features of the cluster even after a period of 30 h. The time dependent MALDI MS data of the decomposition of clusters at 28 °C and 10 °C are shown in Fig. S7†. The cluster solution at 28 °C showed a shift towards the lower mass region indicating decomposition with time. The solution incubated at 10 °C did not show much variation in mass suggesting high stability of the clusters at low temperature.

To further confirm that the mixture of red emitting Ag_{15}@BSA and Ag–BSA conjugate was responsible for the different colours observed under UV light, we conducted an experiment in which different volumes of the initial green emitting Ag–BSA conjugate and red emitting Ag_{15}@BSA were mixed. Solutions of various luminescence colours could be prepared by this method.

The effect of concentration of various reagents on the synthesis of Ag_{15}@BSA was also verified. An increased concentration of BSA (150 mg mL^{-1}) showed a change in luminescence. The observed change was not as remarkable as that in which optimum concentration of BSA was used. Here, the solutions appeared colloidal in nature and also their luminescence was quenched more rapidly. This could be because the luminescence of the clusters formed is masked by the high concentration of the protein present in the solution. Cluster synthesis carried out with a 5 times increased concentration of silver nitrate compared to the optimum concentration also yielded Ag_{15} clusters but further increase in silver concentration did not result in the cluster.

Even though there have been efforts to make protein encapsulated luminescent noble metal clusters,[6,17–22,24] this is the first time a silver quantum cluster with defined nuclearity is prepared in protein confinement. We note here that an Au_{25} core has been reported in BSA[17] and lactoferrin[18] protected clusters and Au_{38} core was seen for clusters synthesised by BSA induced core etching.[6] The previously reported synthetic procedures for protein stabilized noble metal clusters are time consuming and they follow highly sensitive reaction conditions such as temperature, concentrations of ingredients, *etc.* Also the stability of those clusters is restricted to certain temperature, time, and pH. The method described in this paper gives Ag_{15}@BSA at room temperature within one minute. These clusters are stable in a wide pH window of 1 to 12 and also can be preserved in the solid state. The extra stability, better quantum yield, monodispersity and defined nuclearity make our material novel.

Conclusion

In summary, we present a rapid, room-temperature synthetic protocol to make bovine serum albumin protected quantum clusters of silver. The resulting bright red emitting clusters were tentatively assigned as Ag_{15}@BSA based on MALDI MS data. The as-synthesized, water soluble, bright, red emitting clusters showed a peak maximum at 685 nm in aqueous solutions. The chemical composition of these clusters was characterized using MALDI MS, XPS, and EDAX. These clusters were stable for a wide pH range of 1–12. They showed an emission peak at 740 nm in the solid state. We found that the stability of these clusters can be enhanced by the addition of PVP. By controlled addition of the reducing agent, it was possible to tune the observed luminescence of the solutions under UV light from green to red in the visible spectrum. The formation mechanism of the cluster involves an Ag–BSA conjugate and its subsequent reduction. The coexistence of these two materials leads to variation of colours of their mixtures under UV light. The clusters decompose back to the conjugate over a period of several hours at room temperature, generating the same set of colours. Stability of these clusters could be enhanced by keeping the solution at low temperature or in the solid state at room temperature or by the use of stabilizing agents. High yield synthesis and exciting photophysical properties make our new material interesting. Such biocompatible clusters may find applications in biolabeling and imaging.

Acknowledgements

We thank Department of Science and Technology, Government of India for constantly supporting our research program on nanomaterials. Authors thank P. L. Xavier, Nirmal Goswami, and Prof. S. K. Pal for the lifetime measurements.

References

1 M. A. H. Muhammed and T. Pradeep, in *Advanced Fluorescence Reporters in Chemistry and Biology II*, ed. A. P. Demchenko, Springer-Verlag Berlin, Heidelberg, 2010, vol. 9, part 4, pp. 333–353, and references cited therein.
2 I. Diez and R. H. A. Ras, *Nanoscale*, 2011, **3**, 1963–1970, and references cited therein.
3 B. Yoon, H. Hakkinen, U. Landman, A. S. Worz, J.-M. Antonietti, S. p. Abbet, K. Judai and U. Heiz, *Science*, 2005, **307**, 403–407, and the references cited therein.
4 M. Turner, V. B. Golovko, O. P. H. Vaughan, P. Abdulkin, A. Berenguer-Murcia, M. S. Tikhov, B. F. G. Johnson and R. M. Lambert, *Nature*, 2008, **454**, 981–983.
5 A. Sanchez, S. Abbet, U. Heiz, W. D. Schneider, H. Haekkinen, R. N. Barnett and U. Landman, *J. Phys. Chem. A*, 1999, **103**, 9573–9578.
6 M. A. Habeeb Muhammed, P. K. Verma, S. K. Pal, A. Retnakumari, M. Koyakutty, S. Nair and T. Pradeep, *Chem.–Eur. J.*, 2010, **16**, 10103–10112.
7 J. Yu, S. Choi and R. M. Dickson, *Angew. Chem., Int. Ed.*, 2009, **48**, 318–320.
8 C. A. J. Lin, T. Y. Yang, C. H. Lee, S. H. Huang, R. A. Sperling, M. Zanella, J. K. Li, J. L. Shen, H. H. Wang, H. I. Yeh, W. J. Parak and W. H. Chang, *ACS Nano*, 2009, **3**, 395–401.

View Online

9 J. Sharma, H.-C. Yeh, H. Yoo, J. H. Werner and J. S. Martinez, *Chem. Commun.*, 2010, **46**, 3280–3282.
10 A. Retnakumari, S. Setua, D. Menon, P. Ravindran, H. Muhammed, T. Pradeep, S. Nair and M. Koyakutty, *Nanotechnology*, 2010, **21**, 055103.
11 T. Vosch, Y. Antoku, J.-C. Hsiang, C. I. Richards, J. I. Gonzalez and R. M. Dickson, *Proc. Natl. Acad. Sci. U. S. A*, 2007, **104**, 12616–12621.
12 J. M. Slocik and D. W. Wright, *Biomacromolecules*, 2003, **4**, 1135–1141.
13 N. Cathcart, P. Mistry, C. Makra, B. Pietrobon, N. Coombs, M. Jelokhani-Niaraki and V. Kitaev, *Langmuir*, 2009, **25**, 5840–5846.
14 T. U. B. Rao, B. Nataraju and T. Pradeep, *J. Am. Chem. Soc.*, 2010, **132**, 16304–16307.
15 B. Adhikari and A. Banerjee, *Chem. Mater.*, 2010, **22**, 4364–4371.
16 S. I. Tanaka, J. Miyazaki, D. K. Tiwari, T. Jin and Y. Inouye, *Angew. Chem., Int. Ed.*, 2011, **50**, 431–435.
17 J. Xie, Y. Zheng and J. Y. Ying, *J. Am. Chem. Soc.*, 2009, **131**, 888–889.
18 P. L. Xavier, K. Chaudhari, P. K. Verma, S. K. Pal and T. Pradeep, *Nanoscale*, 2010, **2**, 2769–2776.
19 C. Shao, B. Yuan, H. Wang, Q. Zhou, Y. Li, Y. Guan and Z. Deng, *J. Mater. Chem.*, 2011, **21**, 2863–2866.
20 H. Wei, Z. Wang, L. Yang, S. Tian, C. Hou and Y. Lu, *Analyst*, 2010, **135**, 1406–1410.
21 F. Wen, Y. Dong, L. Feng, S. Wang, S. Zhang and X. Zhang, *Anal. Chem.*, 2011, **83**, 1193–1196.
22 H. Liu, X. Zhang, X. Wu, L. Jiang, C. Burda and J.-J. Zhu, *Chem. Commun.*, 2011, **47**, 4237–4239.
23 I. Diez, M. Pusa, S. Kulmala, H. Jiang, A. Walther, A. S. Goldmann, A. H. E. Mueller, O. Ikkala and R. H. A. Ras, *Angew. Chem., Int. Ed.*, 2009, **48**, 2122–2125.
24 S. Liu, F. Lu and J.-J. Zhu, *Chem. Commun.*, 2011, **47**, 2661–2663.
25 C. I. Richards, J. C. Hsiang, D. Senapati, S. Patel, J. Yu, T. Vosch and R. M. Dickson, *J. Am. Chem. Soc.*, 2009, **131**, 4619–4621.
26 Z. Huang, F. Pu, D. Hu, C. Wang, J. Ren and X. Qu, *Chem.–Eur. J.*, 2011, **17**, 3774–3780.
27 W. Guo, J. Yuan, Q. Dong and E. Wang, *J. Am. Chem. Soc.*, 2010, **132**, 932–934.
28 H. Xu and K. S. Suslick, *Adv. Mater.*, 2010, **22**, 1078–1082, and references cited therein.
29 W. Harbich, S. Fedrigo and J. Buttet, *Chem. Phys. Lett.*, 1992, **195**, 613–617.
30 W. Schulze, I. Rabin and G. Ertl, *ChemPhysChem*, 2004, **5**, 403–407.
31 A. D. Stevens and M. C. R. Symons, *J. Chem. Soc., Faraday Trans. 1*, 1989, **85**, 1439–1450.
32 M. Treguer, F. Rocco, G. Lelong, N. A. Le, T. Cardinal, A. Maali and B. Lounis, *Solid State Sci.*, 2005, **7**, 812–818.
33 H. Xu and K. S. Suslick, *ACS Nano*, 2010, **4**, 3209–3214.
34 A. Ledo-Suarez, J. Rivas, C. Rodriguez-Abreu, M. J. Rodriguez, E. Pastor, A. Hernandez-Creus, S. B. Oseroff and M. A. Lopez-Quintela, *Angew. Chem., Int. Ed.*, 2007, **46**, 8823–8827.
35 J. Zhang, S. Xu and E. Kumacheva, *Adv. Mater.*, 2005, **17**, 2336–2340.
36 K. V. Mrudula, T. U. Bhaskara Rao and T. Pradeep, *J. Mater. Chem.*, 2009, **19**, 4335–4342.
37 T. Udaya Bhaskara Rao and T. Pradeep, *Angew. Chem., Int. Ed.*, 2010, **49**, 3925–3929.
38 M. J. Meziani, H. W. Rollins, L. F. Allard and Y.-P. Sun, *J. Phys. Chem. B*, 2002, **106**, 11178–11182.
39 A. Housni, M. Ahmed, S. Liu and R. Narain, *J. Phys. Chem. C*, 2008, **112**, 12282–12290.
40 E. S. Shibu and T. Pradeep, *Chem. Mater.*, 2011, **23**, 989–999.
41 M. A. Habeeb Muhammed and T. Pradeep, *Small*, 2011, **7**, 204–208.
42 J. Xie, J. Y. Lee, D. I. C. Wang and Y. P. Ting, *ACS Nano*, 2007, **1**, 429–439.
43 E. S. Shibu, M. A. Habeeb Muhammed, T. Tsukuda and T. Pradeep, *J. Phys. Chem. C*, 2008, **112**, 12168–12176.
44 R. Chan, V. Chen and M. P. Bucknall, *Biotechnol. Bioeng.*, 2004, **85**, 190–201.
45 O. N. Metin and S. OÌzkar, *Energy Fuels*, 2009, **23**, 3517–3526.
46 L. S. Ott, B. J. Hornstein and R. G. Finke, *Langmuir*, 2006, **22**, 9357–9367.
47 P. Ramasamy, S. Guha, E. S. Shibu, T. S. Sreeprasad, S. Bag, A. Banerjee and T. Pradeep, *J. Mater. Chem.*, 2009, **19**, 8456–8462.

Downloaded by Indian Institute of Technology Chennai on 11 September 2011
Published on 23 June 2011 on http://pubs.rsc.org | doi:10.1039/C1JM11452B

 This journal is © The Royal Society of Chemistry 2011